

# Low-Power Picosecond Resonance Raman Evidence for Histidine Ligation to Heme $a_3$ after Photodissociation of CO from Cytochrome $c$ Oxidase

Johannes P. M. Schelvis,<sup>†</sup> Geurt Deinum,<sup>†,§</sup> Constantinos A. Varotsis,<sup>‡</sup> Shelagh Ferguson-Miller,<sup>†</sup> and Gerald T. Babcock<sup>\*,†</sup>

Contribution from the Department of Chemistry, LASER Laboratory, and Department of Biochemistry, Michigan State University, East Lansing, Michigan 48824, and Department of Chemistry, University of Crete, 71409, Iraklion, Crete, Greece

Received December 2, 1996. Revised Manuscript Received March 14, 1997<sup>⊗</sup>

**Abstract:** Several models have been proposed for the ligand dynamics in the heme  $a_3^{2+}/\text{Cu}_B^{1+}$  binuclear pocket in cytochrome oxidase following CO photodissociation. These range from straightforward heme pocket relaxation to a variety of ligand exchange processes that have been proposed to be of relevance to the proton pumping function of the enzyme. To provide discrimination between these models, we have used picosecond time-resolved, pump–probe resonance Raman spectroscopy to study the photolysis process in the enzyme isolated from beef heart and from *Rhodobacter sphaeroides*. The intermediate observed within 5 ps of photolysis with low-energy probe pulses (10–20 nJ/pulse) is the high-spin, five-coordinate heme  $a_3^{2+}$  to which a histidine is ligated, as indicated by the observation of the Fe-His vibration at 220  $\text{cm}^{-1}$ . Several control experiments demonstrate that the probe pulse energy is sufficiently low to avoid promoting any significant photochemistry during the spectral acquisition phase of the pump–probe experiment. From these observations, we conclude that histidine is ligated to high-spin heme  $a_3^{2+}$  on the picosecond time scale following photolysis. Since H376 is the proximal  $a_3^{2+}$  ligand in the CO complex, our results indicate that this proximal ligation survives photolysis and that the control of the access of exogenous ligands to the heme  $a_3$  site by means of a ligand exchange process can be ruled out. We observe similar picosecond transient resonance Raman spectra for the CO complex of *Rb. sphaeroides* cytochrome  $c$  oxidase. From these results and earlier time-resolved Raman and FTIR measurements, we propose a model for the relaxation dynamics of the heme  $a_3$  pocket that involves picosecond migration of CO to the  $\text{Cu}_B$  center and relaxation of the  $a_3^{2+}$ -proximal histidine bond on the microsecond time scale following CO photolysis.

## Introduction

Cytochrome  $c$  oxidase (CcO) is the terminal electron acceptor in the mitochondrial respiratory chain (see ref 1 for recent reviews). The enzyme contains four redox active metal sites: heme  $a$ , heme  $a_3$ ,  $\text{Cu}_A$ , and  $\text{Cu}_B$ . Molecular  $\text{O}_2$ , which is the final electron acceptor, is bound and reduced at the  $a_3/\text{Cu}_B$  binuclear active site. In addition to its electron transfer and dioxygen reduction functions, cytochrome oxidase also functions as a proton pump and uses the free energy released during  $\text{O}_2$  reduction to translocate protons across the mitochondrial membrane.

Time-resolved spectroscopies have been used to study the reaction of  $\text{O}_2$  with the enzyme and considerable insight into mechanism has resulted.<sup>1b,c,f</sup> Nonetheless, it is sometimes difficult to study ligand binding and coordination chemistry in the binuclear center by using only  $\text{O}_2$  as the ligating species, owing to its high reactivity with the enzyme (turnover rate about 1000 electron  $\text{s}^{-1}$ ). Other exogenous ligands such as CO,  $\text{CN}^-$ ,

and NO often can be used more effectively for this purpose. CO, in particular, which forms a stable complex with the fully reduced enzyme,<sup>2</sup> has been used in time-resolved experiments to investigate the relaxation kinetics at the active site after its photodissociation. The relevance of such measurements has become especially clear recently, as distal ligand exchange mechanisms for coupling proton translocation to redox and coordination events in the binuclear center are currently under active investigation.<sup>3,4</sup>

Alben and co-workers<sup>5</sup> showed that CO transiently binds to  $\text{Cu}_B$  after it has been photodissociated from heme  $a_3$ . Woodruff and co-workers<sup>6</sup> subsequently performed an incisive and detailed study of the kinetics of CO photodissociation. From their results, it is clear that CO dissociates from heme  $a_3$  within 100

(2) (a) Greenwood, C.; Gibson, Q. H. *J. Biol. Chem.* **1967**, *242*, 1782–1787. (b) Yoshikawa, S.; Choc, M. G.; O'Toole, M. C.; Caughey, W. S. *J. Biol. Chem.* **1977**, *252*, 5498–5508.

(3) (a) Wikström, M.; Bogachev, A.; Finel, M.; Morgan, J. E.; Puustinen, A.; Raitio, M.; Verkhovskaya, M. I.; Verkhovsky, M. I. *Biochim. Biophys. Acta* **1994**, *1187*, 106–111. (b) Morgan, J. E.; Verkhovsky, M. I.; Wikström, M. *J. Bioenerg. Biomembr.* **1994**, *26*, 599–608.

(4) Iwata, S.; Ostermeier, C.; Ludwig, B.; Michel, H. *Nature* **1995**, *376*, 660–669.

(5) (a) Alben, J. O.; Moh, P. P.; Fiamingo, F. G.; Altschuld, R. A. *Proc. Natl. Acad. Sci. U.S.A.* **1981**, *78*, 234–237. (b) Fiamingo, F. G.; Altschuld, R. A.; Moh, P. P.; Alben, J. O. *J. Biol. Chem.* **1982**, *257*, 1639–1650.

(6) (a) Stoutland, P. O.; Lambry, J. C.; Martin, J. L.; Woodruff, W. H. *J. Phys. Chem.* **1991**, *95*, 6406–6408. (b) Dyer, R. B.; Peterson, K. A.; Stoutland, P. O.; Woodruff, W. H. *J. Am. Chem. Soc.* **1991**, *113*, 6276–6277. (c) Dyer, R. B.; Einarsdóttir, Ó; Killough, P. M.; López-Garriga, J. J.; Woodruff, W. H. *J. Am. Chem. Soc.* **1989**, *111*, 7657–7659. (d) Einarsdóttir, Ó; Dyer, R. B.; Lemon, D. D.; Killough, P. M.; Hubig, S. M.; Atherton, S. J.; López-Garriga, J. J.; Palmer, G.; Woodruff, W. H. *Biochemistry* **1993**, *32*, 12013–12024.

<sup>†</sup> Michigan State University.

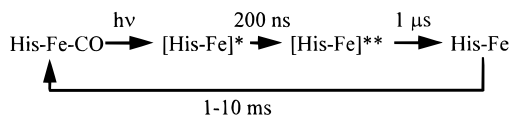
<sup>‡</sup> University of Crete.

<sup>§</sup> Present address: G. R. Harrison Spectroscopy Laboratory, Massachusetts Institute of Technology, Cambridge, MA 02139.

\* To whom correspondence should be addressed.

<sup>⊗</sup> Abstract published in *Advance ACS Abstracts*, August 1, 1997.

(1) (a) Trumpower, B. L.; Gennis, R. B. *Annu. Rev. Biochem.* **1994**, *63*, 675–716. (b) Kitagawa, Y.; Ogura, T. *Prog. Inorg. Chem.* **1996**, *45*, 431–479. (c) Ferguson-Miller, S.; Babcock, G. T. *Chem. Rev.* **1996**, *96*, 2889–2907. (d) Babcock, G. T.; Wikström, M. *Nature* **1992**, *356*, 301–309. (e) Ferguson-Miller, S., Ed. Minireview Series: Cytochrome Oxidase. *J. Bioenerg. Biomembr.* **1993**, *25*. (f) Sucheta, A.; Georgiadis, K. E.; Einarsdóttir, Ó. *Biochemistry* **1997**, *36*, 554–565.

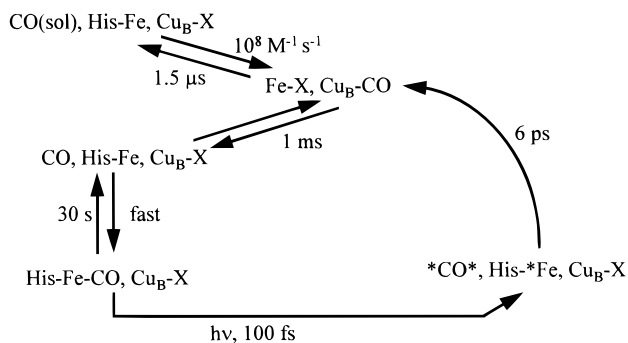
**Scheme 1.** Model of Findsen et al.<sup>10</sup>

fs following excitation<sup>6a</sup> and subsequently binds to Cu<sub>B</sub> in less than 1 ps.<sup>6b</sup> The Cu<sub>B</sub>-CO complex has a half-life of about 1.5 μs,<sup>6c</sup> after which CO leaves the heme a<sub>3</sub> pocket and equilibrates with the solvent. The nongeminate rebinding of CO to heme a<sub>3</sub> occurs through Cu<sub>B</sub> in a process that depends on the CO concentration and occurs on the millisecond time scale.<sup>6d</sup> Although the CO kinetics upon photolysis seem to be understood, no consensus has been reached on the dynamics and coordination chemistry in the heme a<sub>3</sub> pocket after CO photolysis.

One of the key parameters used to investigate the relaxation dynamics of the heme a<sub>3</sub> pocket has been the Fe-His vibration that can be detected by Raman spectroscopy. In the fully reduced enzyme this vibration is observed at a frequency of 212–215 cm<sup>-1</sup>.<sup>7,8</sup> However, when CO binds to heme a<sub>3</sub> to form the six-coordinate CO complex, the Fe-His vibration is no longer observed with Soret excitation. Upon photodissociation of CO, the Fe-His vibration appears at a higher frequency at 220–222 cm<sup>-1</sup><sup>9–13</sup> and relaxes to its equilibrium frequency with a time constant of about 1 μs.<sup>10,13</sup> However, two groups have recently claimed the absence<sup>12</sup> or attenuation<sup>13</sup> of the Fe-His vibration in time-resolved resonance Raman spectra taken at low probe powers after CO photolysis. Three different models have been invoked to explain all or part of these data.

The first model was proposed by Findsen et al.<sup>10</sup> and was based on time-resolved resonance Raman spectroscopy on the nanosecond time scale with high-power probe-pulses (Scheme 1). After photodissociation of CO, the heme macrocycle was proposed to relax on the sub-nanosecond time scale, while the heme pocket remains in a nonequilibrium conformation. These authors concluded that the heme pocket relaxation is slower and occurs in about 1 μs, as the Fe-His vibration attains its equilibrium frequency. They observed nongeminate rebinding of CO on the millisecond time scale.

A second model was suggested by Woodruff and co-workers<sup>6d,12,14</sup> from time-resolved resonance Raman, time-resolved IR, and transient absorption spectroscopies with high- and low-power probe pulses (Scheme 2). After CO photodissociation, CO binds to Cu<sub>B</sub>, which was postulated to trigger the release of an endogenous ligand from the copper center. This ligand was then proposed to bind to the heme a<sub>3</sub> Fe within 6 ps, breaking the bond between the heme Fe and the proximal histidine. CO subsequently dissociates from Cu<sub>B</sub> and equilibrates with the surrounding solvent. The rate-limiting step in the nongeminate rebinding of CO was proposed to be the

**Scheme 2.** Model of Woodruff and Co-workers<sup>6,12,14</sup>

breaking of the bond between the heme Fe and the endogenous ligand, which was assigned a rate of about 1000 s<sup>-1</sup>. The bond between heme a<sub>3</sub> and the ligand that was formed upon CO photodissociation was supposed to be photolabile, which was used to explain the photoacceleration of CO rebinding and the photosensitivity of the time-resolved resonance Raman spectra. This overall interpretation is referred to as the ligand-shuttle model, since Cu<sub>B</sub> and the endogenous ligand are thought to control the access of exogenous ligands to the heme a<sub>3</sub> site by means of a ligand exchange process. The endogenous ligand was also proposed to be involved in the proton translocating function of the enzyme. This model recently found support from nanosecond Raman spectroscopy with low-power probe pulses.<sup>13</sup>

Along similar lines, a third model has been suggested by Rousseau and co-workers.<sup>15</sup> Instead of the distal pocket ligand shuttle proposed by Woodruff,<sup>14</sup> they suggested that, upon binding CO, the proximal Fe-His bond is replaced by a bond between the heme a<sub>3</sub> Fe and a tyrosine at the proximal side. After CO photolysis, the Tyr remains bound to the heme Fe; the Fe-Tyr bond, however, was proposed to be photolabile. The switching between histidine and tyrosine proximal ligands was thought to have a physiological function in proton translocation. Recent site-directed mutagenesis results, however, have shown that this model is unlikely.<sup>16</sup>

In this paper, we present data on the photodissociation of CO from CcO isolated from beef heart and from *Rb. sphaeroides*. The probe power was low enough to avoid photodissociation of CO and of ligands bound to the heme. The results show a transient species that is created ≤5 ps after CO photolysis and persists on the nanosecond time scale. The low-frequency spectrum of this intermediate has the characteristics of reduced heme a<sub>3</sub><sup>2+</sup>, but with all the modes proportionally reduced in intensity. In this intermediate, the Fe-His frequency is upshifted by 6 cm<sup>-1</sup> from 214 cm<sup>-1</sup> in the equilibrium enzyme to 220 cm<sup>-1</sup>. Our results demonstrate histidine ligation to the a<sub>3</sub> heme within 5 ps after CO photolysis. We argue that it is the proximal histidine that remains ligated to heme a<sub>3</sub> and conclude that a distal ligand shuttle<sup>14</sup> in which an endogenous ligand binds transiently to heme a<sub>3</sub> following CO photolysis does not occur. We propose a new model for the events in the heme a<sub>3</sub> pocket upon CO photodissociation on the basis of these results, the work of Findsen et al.,<sup>10</sup> and the CO kinetics results of Woodruff and co-workers.<sup>6</sup> This model does not involve the displacement of an amino acid in the heme a<sub>3</sub> pocket. Preliminary results have been reported elsewhere.<sup>17</sup>

(7) Van Steelandt-Frentrup, J.; Salmeen, I.; Babcock, G. T. *J. Am. Chem. Soc.* **1981**, *103*, 5981–5982.

(8) Ogura, T.; Hon-Nami, K.; Oshima, T.; Yoshikawa, S.; Kitagawa, T. *J. Am. Chem. Soc.* **1983**, *105*, 7781–7783.

(9) Findsen, E. W.; Ondrias, M. R. *J. Am. Chem. Soc.* **1984**, *106*, 5736–5738.

(10) Findsen, E. W.; Centeno, J.; Babcock, G. T.; Ondrias, M. R. *J. Am. Chem. Soc.* **1987**, *109*, 5367–5372.

(11) Sassaroli, M.; Ching, Y. C.; Argade, P. V.; Rousseau, D. L. *Biochemistry* **1988**, *27*, 2496–2502.

(12) Woodruff, W. H.; Einarsdóttir, Ó.; Dyer, R. B.; Bagley, K. A.; Palmer, G.; Atherton, S. J.; Goldbeck, R. A.; Dawes, T. D.; Kliger, D. S. *Proc. Natl. Acad. Sci. U.S.A.* **1991**, *88*, 2588–2592.

(13) Lou, B. S.; Larsen, R. W.; Chan, S. I.; Ondrias, M. R. *J. Am. Chem. Soc.* **1993**, *115*, 403–407.

(14) Woodruff, W. H. *J. Bioenerg. Biomembr.* **1993**, *25*, 177–188.

(15) Rousseau, D. L.; Ching, Y. C.; Wang, J. *J. Bioenerg. Biomembr.* **1993**, *25*, 165–176.

(16) Mitchell, D. M.; Ädelroth, P.; Hosler, J. P.; Fetter, J. R.; Brzezinski, P.; Pressler, M. A.; Aasa, R.; Malmström, B. G.; Alben, J. O.; Babcock, G. T.; Gennis, R. B.; Ferguson-Miller, S. *Biochemistry* **1996**, *35*, 824–828.

## Experimental Procedures

Cytochrome *c* oxidase (CcO) was isolated from beef heart<sup>18</sup> and from *Rb. sphaeroides* WT strain CY91.<sup>19</sup> The samples were stored in liquid nitrogen until further use. The fully reduced enzyme was prepared by cycling the samples six times between vacuum and Ar. Once under Ar atmosphere, sodium dithionite was added to reduce the enzyme fully. The CO complex of bovine and bacterial CcO was prepared in the same way, but with CO in place of Ar. After the last cycle, the sample was left under a CO atmosphere and a minimal amount of sodium dithionite was added to reduce CcO fully and bind CO. The binding of CO was monitored optically and by the high- and low-frequency resonance Raman spectra. The integrity of the samples during and after the experiments was confirmed optically and by Raman. No sample degradation occurred during the time course of the experiments. The bovine and bacterial samples had concentrations of 100–150 and about 50  $\mu\text{M}$ , respectively.

The picosecond time-resolved resonance Raman experiments were performed on a system consisting of two synchronously pumped, cavity dumped dye lasers as described elsewhere.<sup>20</sup> The 1064 nm output of a Coherent Antares Nd:YAG laser was frequency doubled to 532 nm. Both the fundamental and the second-harmonic beam were focused in a BBO crystal to create the third harmonic at 355 nm. The 532 nm beam was used to pump a Coherent 700 dye laser that was operated with Rhodamine-6G and could be tuned from 570 to 620 nm. The 355 nm beam pumped a second Coherent 700 dye laser, which was operated with Stilbene 3 and was tunable from 425 to 470 nm. The pump laser was used at 592 nm, the maximum of the Q-band transition of CO bound heme  $a_3^{2+}$ , and the probe laser was used at either 428 or 441 nm depending on the experiment. Both dye lasers were operated at a repetition rate of 153 kHz with 5 ps pulses. The pump laser had a power of 5.5 mW, and the probe laser had a power of 2.5 mW. The repetition rate of both dye lasers was such that the illuminated sample volume could be refreshed between flashes. For this purpose, the sample was contained in a sealed spinning cell with a radius of 21 mm, while the cell was rotated at  $5.9 \times 10^3$  rpm. The pump and probe beams were focused in the sample by means of a 25 mm focal length microscope objective to a minimal spot size of about 10  $\mu\text{m}$ . The total illuminated volume was about  $1.6 \times 10^{-3}$  mm<sup>3</sup>.

The scattered light was passed through a dichroic filter (low pass, 515 nm) to suppress light from the pump beam and possible fluorescence from the sample, and its polarization was scrambled. The Raman spectrum was dispersed by a single monochromator (Jobin Yvon HR 640, 2400 grooves/mm grating) and detected with a CCD detector (Princeton Instruments, Model LN/CCD 1152UV). To collect the low-frequency resonance Raman spectra, notch filters (Kaiser Optical Systems) with central wavelengths of 427 or 442 nm were used to reject the Rayleigh line and reflect probe-laser light. During pump–probe experiments, we alternated between pump–probe and probe-only conditions at regular intervals (1–2 min). All experiments were performed at room temperature.

The nanosecond resonance Raman spectra were obtained with 427 nm probe light that was provided by pumping Stilbene 3 with the third-harmonic output (355 nm) of a Quanta Ray DCR-2A Nd:YAG laser. The 532 nm pump beam was the second harmonic from a second Quanta Ray DCR-2A. The scattered light passed through a notch filter and was dispersed by a single monochromator (SPEX 500M) and detected with a N<sub>2</sub>(l)-cooled CCD detector (SPEX SPECTRUM1).

## Results

The low-frequency Raman spectra of fully reduced CcO from beef heart and its CO complex obtained at low probe powers

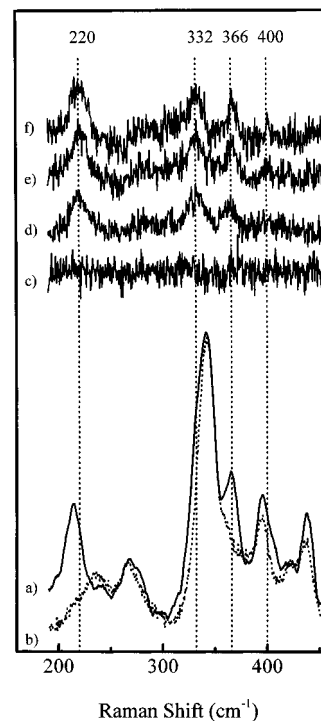


**Figure 1.** Low-frequency resonance Raman spectra of CcO from beef heart: (a) the equilibrium fully reduced enzyme, (b) the CO complex of the fully reduced enzyme (dotted line), (c–f) difference spectra taken 20 ps prior to and 0 ps, 30 ps, and 1 ns after CO photolysis. Spectra a–f were collected on the picosecond laser system with a 441 nm, 2.5 mW probe beam, while for spectra c–f, a 592 nm, 5.5 mW pump beam was used for photolysis. The accumulation time was 5 min each for spectra a–f, and the difference spectra were calculated as described in the text.

are shown in Figure 1. The Raman spectrum of the fully reduced enzyme is characterized by the Fe–His stretching mode at  $214\text{ cm}^{-1}$ <sup>7,8</sup> and porphyrin modes at 340, 366, 394, and  $438\text{ cm}^{-1}$  (Figure 1a).<sup>21–23</sup> The binding of CO to heme  $a_3^{2+}$  is accompanied by disappearance of the Fe–His stretching vibration at  $214\text{ cm}^{-1}$  and of the porphyrin mode at  $366\text{ cm}^{-1}$  and by narrowing of the  $340\text{ cm}^{-1}$  band, which is due to the disappearance of a mode at approximately  $330\text{ cm}^{-1}$  (Figure 1b). These three low-frequency bands, i.e., those at 214, 330, and  $366\text{ cm}^{-1}$ , have previously been assigned to the five-coordinate, high-spin heme  $a_3^{2+}$ <sup>24,25</sup> and are expected to contribute strongly to the Raman difference spectra of the CO complex of fully reduced CcO after photodissociation of CO by a laser pulse.

In Figure 1c–f, we show difference spectra obtained with low probe power taken at 20 ps prior to and 0, 20 ps, and 1 ns after photolysis. The difference spectra were obtained by normalizing pump–probe and probe-only spectra to the  $438\text{ cm}^{-1}$  peak<sup>26</sup> and subtracting the probe-only from the pump–probe spectrum. The difference spectra were scaled by normalizing the individual probe-only spectra to each other. The intermediate that is observed after photodissociation of CO has a low-frequency spectrum that is characterized by three main bands at 220, 332, and  $366\text{ cm}^{-1}$ . Therefore, we identify the

(17) Schelvis, J. P. M.; Deinum, G.; Kim, Y.; Babcock, G. T. In *Fifteenth International Conference on Raman Spectroscopy*; Stein, P., Asher, S. A., Eds.; John Wiley & Sons: New York, 1996; pp 144–145.

(18) Babcock, G. T.; Jean, J. M.; Johnston, L. N.; Palmer, G.; Woodruff, W. H. *J. Am. Chem. Soc.* **1984**, *106*, 8305–8306.

(19) (a) Hosler, J. P.; Fetter, J.; Tecklenburg, M. M. J.; Espe, M.; Lerma, C.; Ferguson-Miller, S. *J. Biol. Chem.* **1992**, *267*, 24264–24272. (b) Mitchell, D. M.; Gennis, R. B. *FEBS Lett.* **1995**, *368*, 148–150.

(20) Krezowski, D. H.; Deinum, G.; Babcock, G. T. *J. Am. Chem. Soc.* **1994**, *116*, 7463–7464.

(21) Choi, S.; Lee, J. J.; Wei, Y. H.; Spiro, T. G. *J. Am. Chem. Soc.* **1983**, *105*, 3692–3707.

(22) Abe, M.; Kitagawa, T.; Kyogoku, Y. *J. Chem. Phys.* **1978**, *69*, 4526–4534.

(23) Choi, S.; Spiro, T. G. *J. Am. Chem. Soc.* **1983**, *105*, 3638–3692.

(24) Salmeen, I.; Rimai, L.; Babcock, G. T. *Biochemistry* **1978**, *17*, 800–806.

(25) (a) Ching, Y. C.; Argade, P. V.; Rousseau, D. L. *Biochemistry* **1985**, *24*, 4938–4946. (b) Argade, P. V.; Ching, Y. C.; Rousseau, D. L. *Biophys. J.* **1986**, *50*, 613–620.

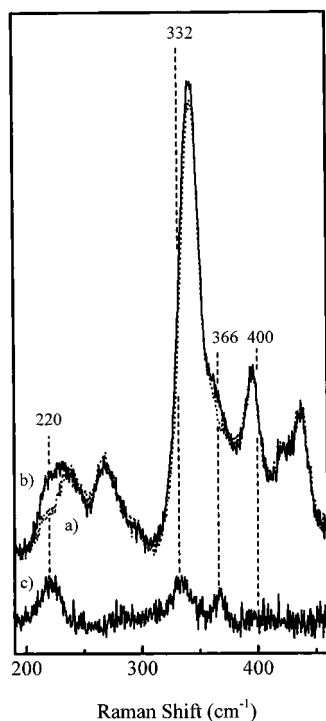


**Figure 2.** Low-frequency resonance Raman spectra of the CO complex of fully reduced CcO from beef heart: (a) the probe-only spectrum (dotted line), (b) the matching pump-probe spectrum collected 40 ps after CO photolysis (solid line), (c) the difference spectrum obtained by subtracting the probe-only spectrum from the pump-probe spectrum as described in the text. The experimental conditions were as described in Figure 1.

intermediate as five-coordinate heme  $a_3^{2+}$ , in which the Fe-His stretch has been upshifted by  $6\text{ cm}^{-1}$ . This result is similar to previous results that have been obtained in high-probe-power experiments with nanosecond pulses.<sup>9–13</sup> In Figure 2, we show the probe-only spectrum of the CO complex (spectrum a, dotted line) and its matching pump-probe spectrum taken 40 ps after photolysis (spectrum b, solid line) together with their difference spectrum (spectrum c, bottom trace). In the high-probe-power, nanosecond experiments, the intensities of the  $a_3^{2+}$  Fe-His and macrocycle modes in the photoproduct are comparable to those in the fully reduced enzyme.<sup>10</sup> By comparing Figure 1a,b with Figure 2a,b, however, it is clear that the Fe-His and macrocycle vibrations of heme  $a_3^{2+}$  in the photoproduct obtained with low probe power are substantially suppressed in intensity relative to the fully reduced protein. This suppression of heme  $a_3^{2+}$  modes in the low-probe-power transient spectrum is not due to a low yield of CO photolysis in our experiments, as we estimate that we achieve about 40% photolysis in our experiments.<sup>27</sup> Thus, the suppression is inherent to the low-probe-power experiment and has been observed by other groups.<sup>12,13</sup> When the pump power was attenuated by a factor of 2.5, the intensity of the  $220\text{ cm}^{-1}$  mode decreased by the same factor, indicating that the pump power was below saturation level.

We also collected the pump-probe spectrum at 10 ns after photolysis with low-probe-power, nanosecond pulses (data not

(26) Picosecond resonance Raman experiments on the fully reduced enzyme showed that neither excitation at 592 nm nor excitation at 605 nm, while probing at 441 nm, induced changes in the resonance Raman spectra (data not shown). Thus, we conclude that heme  $a^{2+}$  modes do not contribute to the picosecond Raman difference spectra of the CO complex. The  $438\text{ cm}^{-1}$  mode originates from heme  $a^{2+}$ , and therefore, normalization to this peak will eliminate all heme  $a$  modes from the difference spectra.

(27) We estimate the percentage of CO photolysis by comparing our pump-probe resonance Raman spectrum (Figure 2b) with the transient resonance Raman spectra of Lou et al. (ref 13, their Figure 1) that are shown as a function of laser energy density, i.e., percentage of CO photolysis.

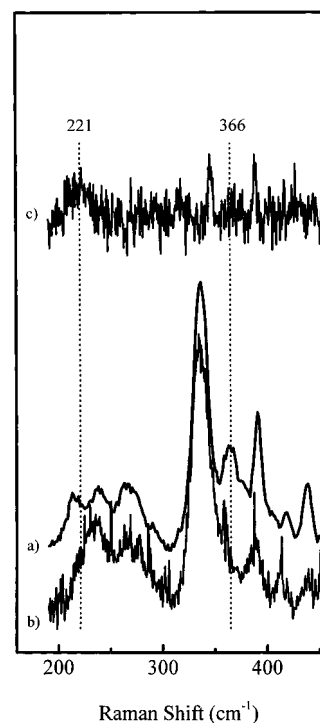


**Figure 3.** Low-frequency resonance Raman spectra of CcO from *Rb. sphaeroides*: (a) the equilibrium fully reduced enzyme, (b) the CO complex of the fully reduced enzyme, (c) difference spectrum 50 ps after CO photolysis by a 592 nm, 5.5 mW excitation beam. Spectra b and c were collected on the picosecond laser system with a 441 nm, 2.5 mW probe beam, while for spectrum c, a 592 nm, 5.5 mW pump beam was used for photolysis. Spectrum a was measured on a nanosecond laser system with a repetition rate of 10 Hz and 0.2 mJ, 427 nm probe pulses. The accumulation time was 15 min for spectrum a, 90 min for spectrum b, and 30 min each for spectrum c.

shown). This spectrum resembles the low-probe-power, 200 ns spectrum shown by Woodruff et al.<sup>12</sup> and our pump-probe spectra (e.g., Figure 2b) on the picosecond time scale, indicating that the low  $a_3^{2+}$  Fe-His and macrocycle mode intensities persist on the sub-microsecond time scale.

Very similar low-probe-power spectra were obtained for CcO isolated from *Rb. sphaeroides* as shown in Figure 3. The low-frequency Raman spectrum of the reduced enzyme is quite similar to that of beef heart reduced CcO (Figure 3a). Again, upon binding CO to the fully reduced enzyme, the vibrations at 214, 330, and  $366\text{ cm}^{-1}$  disappear (Figure 3b). In the difference spectrum obtained 50 ps after CO photodissociation, a band at  $221\text{ cm}^{-1}$  is distinguishable (Figure 3c), analogous to the  $220\text{ cm}^{-1}$  mode observed with the beef heart enzyme. Modes at 330 and  $366\text{ cm}^{-1}$  are not readily apparent, most likely because the Raman cross sections for these modes are decreased in the photoproduct.<sup>28</sup> From the behavior of the  $221\text{ cm}^{-1}$  vibration, we conclude that CcO from *Rb. sphaeroides* behaves in a manner analogous to that of CcO from beef heart after photodissociation of CO. This conclusion is supported by the fact that the recently obtained crystal structures of mammalian<sup>29</sup> and of bacterial<sup>4</sup> CcO are very similar in the binuclear center region in subunit I.

(28) Although the Raman bands for the  $a_3^{2+}$  modes in *Rb. sphaeroides* oxidase occur at essentially identical positions to these in the beef heart enzyme, we have observed in previous work (e.g., ref 19a) that their Raman cross sections vary substantially from those of the mammalian enzyme.

(29) (a) Tsukihara, T.; Aoyama, H.; Yamashita, E.; Tomizaki, T.; Yamaguchi, H.; Shinzawa-Itoh, K.; Nakashima, R.; Yaono, R.; Yoshikawa, S. *Science* **1995**, *269*, 1069–1074. (b) Tsukihara, T.; Aoyama, H.; Yamashita, E.; Tomizaki, T.; Yamaguchi, H.; Shinzawa-Itoh, K.; Nakashima, R.; Yaono, R.; Yoshikawa, S. *Science* **1996**, *272*, 1136–1144.

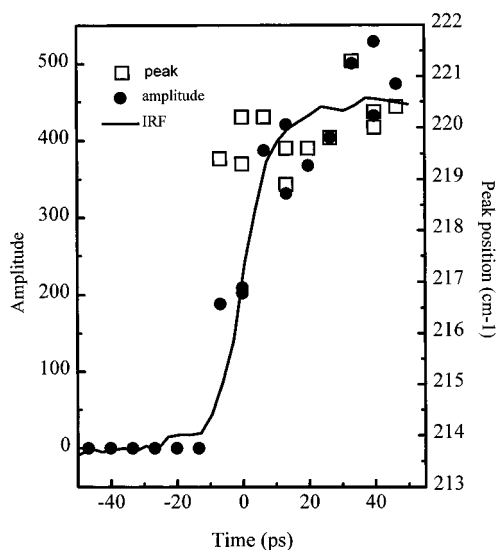


**Figure 4.** Peak position (squares) and amplitude (circles) of the Fe-His vibration of the CO complex of fully reduced CcO as a function of delay time between pump and probe pulses. The instrument response function as monitored with ZnTPP is given by the solid line. The pump (592 nm, 5.5 mW) and probe (441 nm, 2.5 mW) lasers had a repetition rate of 153 kHz. The peak positions and amplitudes were determined as described in the text.

The difference spectra in Figure 1 show that the position of the  $220\text{ cm}^{-1}$  peak does not relax on the nanosecond time scale with low probe power, which confirms earlier observations by Findsen et al.<sup>10</sup> To define the time scale of the frequency upshift immediately following CO photolysis, we investigated the position of this peak around zero delay time in detail with a time resolution of about 5 ps. The position of the peak and its amplitude were determined by fitting a Gaussian to part of the difference spectrum from  $175$  to  $245\text{ cm}^{-1}$ , while the difference spectra were calculated as described above. The time delays were chosen in random order to avoid systematic errors that might occur from unidirectionally changing the optical delay line. The position of the peak (squares) as a function of delay time is shown in Figure 4 together with its amplitude (circles) and the instrument response function (IRF, line), which had been obtained by probing the disappearance of the ground-state Raman spectrum of ZnTPP. Although the amplitude of the peak follows the IRF, the position of the peak is always around  $220\text{ cm}^{-1}$  as soon as it is detectable in the difference spectra. This result indicates that no fast initial relaxation takes place on the picosecond time scale and that the Fe-His frequency upshift occurs within the time resolution of our instrument, i.e., in less than 5 ps.

The picosecond spectra in Figures 1–3 are analogous to nanosecond data in showing a  $220\text{ cm}^{-1}$  Fe-His mode upon CO photolysis. Woodruff and co-workers,<sup>6d,12,14</sup> however, have suggested that the  $220\text{ cm}^{-1}$  mode observed on the nanosecond time scale reflects photolysis of an endogenous ligand (X in Scheme 2) by the nanosecond Raman probe pulse and its subsequent replacement by the proximal histidine. To test the photolytic activity of our picosecond probe, we examined the effect of the probe power on the Raman spectra to be certain that the probe power used for our experiments was low enough to avoid the photolysis of CO. Because the quantum yield for CO photolysis is 1,<sup>30</sup> this experiment also provides a means by which to ascertain whether our probe power is sufficiently low to avoid photolysis of any postulated endogenous ligand bound to heme  $a_3$ . In Figure 5A, the low-frequency Raman spectrum

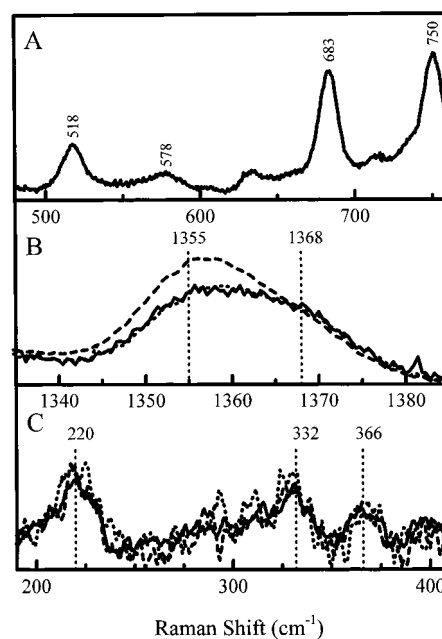


**Figure 5.** (A) Low-frequency resonance Raman spectrum of the CO complex of fully reduced CcO obtained with 428 nm excitation. The probe power was 1.7 mW, and the total accumulation time was 30 min. (B) High-frequency resonance Raman spectra of the CO complex of fully reduced CcO obtained with 441 nm excitation; probe powers are 2.5 mW (dashed line, 10 min), 0.3 mW (solid line, 45 min), and 2.5 mW, but 50 ps following a 592 nm pump beam of 5.5 mW (dashed-dotted line, 10 min). (C) Low-frequency time-resolved resonance Raman spectra of the CO complex of fully reduced CcO collected 50 ps after CO photodissociation by a 592 nm pump (5 mW) with a 441 nm probe with energies of 2.5 mW (solid line, 8 min), 0.8 mW (dashed line, 10.5 min), and 0.6 mW (dotted line, 13.5 min).

of the CO complex of fully reduced CcO obtained with low-power picosecond pulses at the 428 nm Soret maximum of the  $a_3^{2+}$ -CO complex is shown. The energy per probe pulse (11 nJ) is similar to that used in the time-resolved experiments in Figures 1 and 2 when we used 441 nm probe pulses (16 nJ). The fact that we observe the Fe-CO stretching mode at  $518\text{ cm}^{-1}$  and the Fe-C-O bending mode at  $578\text{ cm}^{-1}$ <sup>31</sup> in Figure 5A indicates that our low-energy 428 nm pulses do not cause appreciable CO photolysis of the carbon monoxy complex. The complementary conclusion is that our 441 nm probe pulses are not sufficiently intense to photodissociate postulated endogenous ligands following CO photolysis by the pump, even if the photolysis quantum yield approaches that of the CO complex.

Additional evidence that our probe pulse is sufficiently low in intensity to avoid significant photolysis of putative endogenous ligands is shown in Figure 5B, where we probe the  $\nu_4$  region of the CO complex of fully reduced CcO with 441 nm light. If we use the same probe power as we did in the time-resolved study, we observe a broad  $\nu_4$ . This is in agreement with earlier reports that, in the CO complex of the fully reduced enzyme, the  $\nu_4$  of heme  $a_3$  shifts from  $1355\text{ cm}^{-1}$  to  $1368\text{ cm}^{-1}$ .<sup>25b</sup> If we decrease the probe power by a factor of 10, the  $\nu_4$  line shape persists. This observation shows that our probe power is low enough to avoid CO photodissociation. However, if we use pump pulses as well, we see a clear change in the  $\nu_4$  region (see Figure 5B). The  $1355\text{ cm}^{-1}$  peak sharpens with only a shoulder at  $1368\text{ cm}^{-1}$ , which indicates that our pump power is high enough to photodissociate a significant amount of CO, consistent with our conclusions above.

(30) Gibson, Q. H.; Greenwood, C. *Biochem. J.* **1963**, *86*, 541–554.

(31) Argade, P. V.; Ching, Y. C.; Rousseau, D. L. *Science* **1984**, *225*, 329–331.

In a further investigation of probe-pulse effects, we examined the influence of probe power on the  $220\text{ cm}^{-1}$  vibration observed after photolysis of CO. We used several different probe powers, while keeping the pump power at a fixed energy. In Figure 5C, three difference spectra are shown that were obtained with different probe powers. The difference spectra were obtained and scaled as discussed above for Figure 1. It is clear that decreasing the probe power by a factor of 3 or 4 does not change the relative amplitude of the  $220\text{ cm}^{-1}$  band. This result is consistent with the other experiments in Figure 5 in showing that the probe powers used in the work described here are low enough to avoid the potential photodissociation of a ligand bound to heme  $a_3$  after photolysis of CO. As an additional control, we attenuated the pump power by a factor of 2.5 and observed that the amplitude of the  $220\text{ cm}^{-1}$  band decreased by the same factor (data not shown). This observation indicates that the amplitude of the  $220\text{ cm}^{-1}$  band does depend on the amount of CO photodissociated.

## Discussion

The heme  $a_3$  pocket dynamics upon CO photolysis were initially described in the model proposed by Findsen et al.<sup>10</sup> (Scheme 1). This model was expanded and modified by Woodruff and co-workers<sup>6d,12,14</sup> (Scheme 2), who showed that CO ligates to  $\text{Cu}_B$  after CO photolysis. They also proposed that the protein erects a barrier to CO recombination, which they postulated to be the transfer of an endogenous ligand (X in Scheme 2) to heme  $a_3$ . This ligand binds to heme  $a_3$  on the distal side and ruptures the bond between heme  $a_3$  and the proximal histidine. The ligand switch constitutes a major difference between the two models, since, in the Findsen et al.<sup>10</sup> model, the proximal histidine remains ligated to heme  $a_3$  after CO photolysis. Although the Los Alamos data on the CO kinetics are compelling, no direct observation of the transient ligation of X has been reported. Our study addresses this issue directly, as the combination of low-probe powers and picosecond pulse duration gives us the opportunity to investigate the identity of the ligand bound to heme  $a_3$  immediately after photolysis.

### The Identities of the Photoproduct and Its Axial Ligand.

The bands in the low-frequency time-resolved Raman difference spectra at 220, 332, and  $366\text{ cm}^{-1}$  in Figure 1 can be compared to the spectrum of heme  $a_3^{2+}$ , which shows four modes at 214, 326, 366, and  $400\text{ cm}^{-1}$ .<sup>24,25</sup> The bands at 220 and  $366\text{ cm}^{-1}$  have been observed before in transient and continuous wave (cw) resonance Raman spectra taken after CO photolysis<sup>9–13</sup> and have been assigned to the Fe-His vibration and the  $2\nu_{35}$  porphyrin mode of heme  $a_3^{2+}$ , respectively.<sup>21,23</sup> The third band at  $332\text{ cm}^{-1}$ , has not been reported before in time-resolved experiments, but it aligns with the band at  $326\text{ cm}^{-1}$  in the cw Raman spectrum of heme  $a_3^{2+}$ , which has been assigned to a porphyrin–vinyl bending mode.<sup>25,21,23</sup> From our data, we conclude that its apparent frequency upshift is negligible ( $\leq 2\text{ cm}^{-1}$ ). The difference spectra in Figure 1 show a weak mode at  $400\text{ cm}^{-1}$ , although we cannot assign a peak at that position unambiguously. Taken together, the peak positions in the difference spectra in Figure 1 are analogous to those of the five coordinate, histidine-ligated deoxy  $a_3^{2+}$  species. Moreover, the relative intensities of the Raman bands in the difference spectra seem to be unchanged relative to the deoxy species. By investigating the effect of the probe energies used in our experiments, we showed above that they are sufficiently low to avoid photodissociation of a ligand bound to heme  $a_3^{2+}$  after photolysis. Therefore, we conclude that the photoproduct is the high-spin, five-coordinate heme  $a_3^{2+}$  and that it has a histidine as its axial ligand. The characteristic Fe-His stretching

frequency has been upshifted by  $6\text{ cm}^{-1}$ . The formation of either a 4-coordinated heme species or a 5-coordinated Fe-X species with a Raman silent Fe–X vibration upon photolysis can be ruled out: either of these species lacks the Fe–His vibration, which is expected to increase the relative intensities of the  $a_3^{2+}$  low-frequency macrocycle modes relative to its Fe–His vibration in the Raman difference spectra. Our results, on the contrary, show that the intensities of macrocycle and axial ligand modes are not significantly altered with respect to each other in the photoproduct.

**Proximal vs Distal Ligation.** Our results demonstrate, unambiguously, histidine coordination to the heme  $a_3$  iron upon CO photolysis. Whether this ligating histidine is the proximal residue, which survives photolysis, or a distal residue operating in a ligand shuttle mode can now be considered. If the ligand shuttle is operative, then X in Scheme 2 must be identified with a histidyl ligand to  $\text{Cu}_B$ . It is known that  $\text{Cu}_B$  is ligated by three histidines,<sup>1a,29,4,32</sup> one of which does appear to undergo coordination changes in different forms of the enzyme.<sup>4,29</sup> From the crystal structure, it seems that the distance between these histidines and heme  $a_3$  is too large<sup>29</sup> to allow one of them to act transiently as an Fe ligand. The  $\text{Cu}_B$  site is conformationally flexible,<sup>5</sup> however, and therefore the crystallographic distance may be misleading under dynamic conditions. Gardner et al. have argued recently, for example, that shifts in the position of  $\text{Cu}_B$  relative to heme  $a_3$ , and accordingly also its ligands, must occur to accommodate the range of exogenous distal ligands that bind the  $a_3$  center.<sup>33</sup> Thus, motion and exchange of one of the  $\text{Cu}_B$  histidine ligands is a distinct possibility. This possibility is reinforced by recent experiments in the myoglobin mutant, H93G, in which the proximal histidine has been replaced by glycine. In this engineered protein, the distal histidine ligates the heme, which demonstrates that distal residues can bridge relatively large distances to ligate heme Fe under certain conditions.<sup>34</sup>

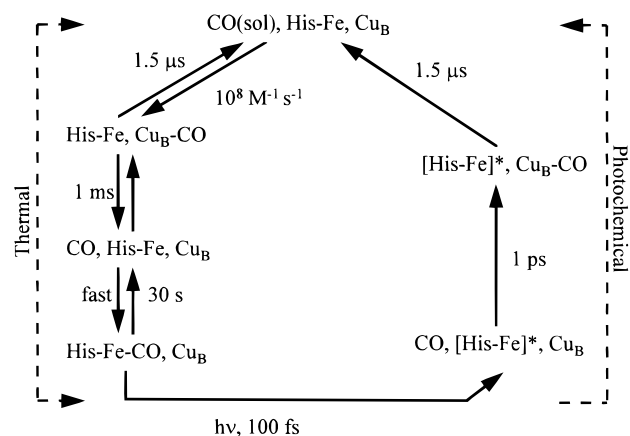
Several arguments, however, suggest that such a distal ligation scenario does not occur transiently in cytochrome oxidase upon CO photolysis. First, a distal ligation process requires significant protein rearrangement and it is unlikely to occur on the  $\leq 5\text{ ps}$  time scale that we have established for the appearance of the Fe-His mode in the CO photolysis product. Second, the similarity of the low-frequency spectra under low- and high-probe-power conditions and the presence of the frequency-upshifted Fe-His mode at zero delay time argue in favor of proximal histidine ligation. Finally, the original observations that led to the ligand shuttle model, i.e., the reduced intensity of the Fe-His mode in the photoproduct<sup>12,35</sup> and its photosensitivity to high probe powers,<sup>12,13</sup> can be accounted for within the context of proximal histidine ligation in the initial photolysis intermediate (see below). Taken together, these considerations provide solid support for persistent proximal histidine ligation upon CO photolysis and argue strongly against the more radical alternative of a distal histidine-based ligand shuttle.

(32) Hosler, J. P.; Ferguson-Miller, S.; Calhoun, M. W.; Thomas, J. W.; Hill, J.; Lemieux, L.; Ma, J.; Georgiou, C.; Fetter, J.; Shapleigh, J.; Tecklenburg, M. M. J.; Babcock, G. T. B.; Gennis, R. B. *J. Bioenerg. Biomembr.* **1993**, *25*, 121–136.

(33) Gardner, M. T.; Deinum, G.; Kim, Y.; Babcock, G. T.; Scott, M. J.; Holm, R. H. *Inorg. Chem.* **1996**, *35*, 6878–6884.

(34) (a) Franzen, S.; Decatur, S. M.; Boxer, S. G.; Dyer, R. B.; Woodruff, W. H. In *Fifteenth International Conference on Raman Spectroscopy*; Stein, P., Asher, S. A., Eds.; The McGraw-Hill Co., Inc., College Custom Series: New York, 1996; Vol. II, pp 66–67. (b) Franzen, S.; Decatur, S. M.; Boxer, S. G.; Dyer, R. B.; Woodruff, W. H. Manuscript in preparation.

(35) Consistent with the uniform reduction in the intensities of the  $a_3^{2+}$  modes upon CO photolysis that we report here, the earlier work showed significant reduction in the intensity of the  $366\text{ cm}^{-1}$   $a_3^{2+}$  macrocycle vibration along with the attenuation of the Fe-His intensity in the photoproduct (cf. Figure 1 in ref 12).

**Scheme 3.** New Model for CO Kinetics, Heme-Pocket Relaxation, and Coordination Chemistry in the Heme  $a_3$  Pocket**CO Photolysis and Heme Pocket Dynamics in Cytochrome**

**$c$  Oxidase.** In Scheme 3, we present a model that combines the Findsen et al.<sup>10</sup> model with the CO kinetics data of Woodruff and co-workers<sup>6</sup> and integrates the new insights gained from the present work. The model consists of two branches for CO ligation dynamics at the  $a_3$  site, one thermal and the other photochemical. The thermal branch describes the equilibrium kinetics of (re)binding and dissociation of CO to and from  $Cu_B$  and heme  $a_3$ . This part is similar to the Woodruff model<sup>14</sup> except that we have eliminated the distal ligand shuttle as providing a barrier to CO recombination at  $a_3$  and that we discriminate between two different  $Cu_B$ -CO complexes: one that is part of the thermal branch with the heme  $a_3$  pocket relaxed and the other in the photochemical branch, in which the pocket is not at thermal equilibrium. In the photochemical branch, CO dissociates from heme  $a_3$  within 100 fs after excitation<sup>6a</sup> and binds to  $Cu_B$  in about 1 ps.<sup>6b</sup> The heme  $a_3$  pocket is left in a nonequilibrium conformation with the proximal histidine ligated to heme  $a_3$ . Findsen et al. showed that the heme pocket relaxes to its equilibrium conformation with a time constant of about 1.5  $\mu$ s.<sup>10</sup> As the data in Figure 1 show that the upshift in Fe-His frequency after CO photolysis is independent of probe intensity, we have retained this half time. On the same time scale, CO dissociates from  $Cu_B$  and equilibrates into the surrounding solvent.<sup>6c</sup> Nongeminate rebinding of CO occurs through the thermal branch on the ms time scale.<sup>10,6d</sup>

**Exogenous Ligand Binding Constants.** In Scheme 3, we have excluded the distal ligation barrier to CO to account for its slow (re)binding kinetics, as discussed above. Additional support for the absence of rate-limiting dissociation of a distal ligand is the fact that ligation barriers do not occur for other exogenous ligands;  $O_2$  and NO, for example, show binding kinetics on the ms and ns time scale, respectively, following CO photodissociation.<sup>36</sup> In this regard, cytochrome oxidase resembles myoglobin, hemoglobin, cytochrome  $c$  peroxidase and P450<sub>cam</sub>, all of which also bind CO much more slowly than NO or  $O_2$ .<sup>37,1d</sup> In fact, the CO association rate constant in

oxidase ( $7 \times 10^4 \text{ M}^{-1} \text{ s}^{-1}$ ) is significantly faster than that in cytochrome  $c$  peroxidase ( $2 \times 10^3 \text{ M}^{-1} \text{ s}^{-1}$ ) and comparable to that in P450<sub>cam</sub> ( $4 \times 10^4 \text{ M}^{-1} \text{ s}^{-1}$ ).<sup>1d</sup> The basis for protein control of ligand association constants in heme proteins may be related to three, ligand-specific factors: (a) electronic barriers imposed by spin state restrictions on binding constants, (b) steric and electrostatic constraints in the distal pocket, and (c) redox processes involving the bound ligand. In hemoglobin, the first two factors have been extensively discussed in rationalizing differences in rebinding processes for CO, NO, and  $O_2$  following ligand dissociation.<sup>37a,c,e,38</sup> Differential barriers to fast geminate recombination are usually attributed to spin state effects, whereas ligand selectivity in nongeminate ligand association are linked to distal pocket effects. Mutagenesis studies on hemoglobin and myoglobin,<sup>39</sup> and experiments with heme models,<sup>40</sup> have shown that local electrostatic interactions between the distal pocket and the ligand can significantly influence association rate constants and binding affinities of small exogenous ligands. We have discussed these recently in considering exogenous ligand selectivity in the NO-activated heme protein, guanylate cyclase.<sup>41</sup>

In cytochrome oxidase, similar electronic and distal pocket effects are undoubtedly at work. In the case of CcO, however, the presence of  $Cu_B$  in the distal heme-pocket significantly affects the (re)binding process; recent work<sup>6d,42,43</sup> has shown that the preequilibration of CO with  $Cu_B$  (Scheme 3) contributes in influencing CO binding kinetics. As we will discuss in detail elsewhere,<sup>44</sup> this small molecule/ $Cu_B$  preequilibrium is ligand specific and can account for the additional selectivity with which cytochrome oxidase binds its physiological dioxygen substrate relative to CO.

**Enhancement of the Fe-His and Heme  $a_3^{2+}$  Modes.** There is a significant reduction in relative scattering cross-sections for the low-frequency heme  $a_3^{2+}$  modes in the Raman spectrum of the photoproduct when low-energy probe pulses (Figures 1 and 2, and ref 13), rather than higher-energy probe pulses,<sup>12,13</sup> are used to interrogate the transient species. This reduction has been explained by the transient binding of a photolabile endogenous ligand to heme  $a_3$  following CO photolysis.<sup>12</sup> Our results, however, are clearly inconsistent with the transient binding of such a ligand. An alternative explanation for the observed probe-power dependence of the intensities of the  $a_3^{2+}$  Fe-His vibration and its low-frequency macrocycle modes may be that two slightly different conformational states of the photoproduct are involved. Transient absorption experiments by several groups have shown different absorption spectra of

(38) (a) Green, B. I.; Hochstrasser, R. M.; Weisman, R. B.; Eaton, W. A. *Proc. Natl. Acad. Sci. U.S.A.* **1978**, *75*, 5255–5259. (b) Chernoff, D. A.; Hochstrasser, R. M.; Steele, A. W. *Proc. Natl. Acad. Sci. U.S.A.* **1980**, *77*, 5606–5610. (c) Friedman, J. M.; Scott, T. W.; Stepnoski, R. A.; Ikeda-Saito, M.; Yonetani, T. *J. Biol. Chem.* **1983**, *258*, 10564–10572. (d) Martin, J. L.; Migus, A.; Poyart, C.; Lecarpentier, Y.; Astier, R.; Antonetti, A. *Proc. Natl. Acad. Sci. U.S.A.* **1983**, *80*, 173–177.

(39) (a) Scott, T. W.; Friedman, J. M.; MacDonald, V. W. *J. Am. Chem. Soc.* **1985**, *107*, 3702–3705. (b) Springer, B. A.; Sliger, S. G.; Olson, J. S.; Phillips, G. N., Jr. *Chem. Rev.* **1994**, *94*, 699–714. (c) Petrich, J. W.; Lambry, J. C.; Balasubramanian, S.; Lambright, D. G.; Boxer, S. G.; Martin, J. L. *J. Mol. Biol.* **1994**, *238*, 437–444.

(40) (a) Traylor, T. G.; Koga, N.; Deardurff, L. A. *J. Am. Chem. Soc.* **1985**, *107*, 6504–6510. (b) Rose, E.; Boitrel, B.; Quelquejeu, M.; Kossanyi, A. *Tetrahedron Lett.* **1993**, *34*, 7267–7270.

(41) (a) Deinum, G.; Stone, J. R.; Babcock, G. T.; Marletta, M. A. *Biochemistry* **1996**, *35*, 1540–1547. (b) Kim, S.; Deinum, G.; Gardner, M. G.; Marletta, M. A.; Babcock, G. T. *J. Am. Chem. Soc.* **1996**, *118*, 8769–8770.

(42) Lemon, D. D.; Calhoun, M. W.; Gennis, R. B.; Woodruff, W. H. *Biochemistry* **1993**, *32*, 11953–11956.

(43) Mitchell, R.; Moody, A. J.; Rich, P. R. *Biochemistry* **1995**, *34*, 7576–7585.

(44) Schelvis, J. P. M.; Babcock, G. T.; Ferguson-Miller, S. Manuscript in preparation.

(36) Blackmore, R. S.; Greenwood, C.; Gibson, Q. H. *J. Biol. Chem.* **1991**, *266*, 19245–19249.

(37) (a) Austin, R. H.; Beeson, K. W.; Eisenstein, I.; Frauenfelder, H.; Gunsalus, I. C. *Biochemistry* **1975**, *14*, 5255–5373. (b) Lim, M.; Jackson, T. A.; Anfirud, P. A. *Proc. Natl. Acad. Sci. U.S.A.* **1993**, *90*, 5801–5804. (c) Petrich, J. W.; Poyart, C.; Martin, J. L. *Biochemistry* **1988**, *27*, 4049–4060. (d) Cornelius, P. A.; Steele, A. W.; Chernoff, D. A.; Hochstrasser, R. M. *Proc. Natl. Acad. Sci. U.S.A.* **1981**, *78*, 7526–7529. (e) Cornelius, P. A.; Hochstrasser, R. M.; Steele, W. A. *J. Mol. Biol.* **1983**, *163*, 119–128.

the photoproduct,<sup>6a,d,45,46</sup> which suggests that two different conformational states exist. If the Raman cross section of the photoproduct is different for its two conformational states, then the probe-power dependence of the Fe-His intensity may be explained by the transition from one conformational state to the other at high probe powers. Transient absorption studies on myoglobin and hemoglobin suggest that in the photolysis product in these systems the heme is also in a slightly different conformational state with respect to the equilibrium deoxy species.<sup>47,37c,38b</sup> In agreement with our analysis, recent experiments on myoglobin showed that porphyrin modes lose significant intensity, when the Soret band shifts to the red in the photoproduct upon CO photolysis.<sup>48</sup>

**Nature of the Frequency Upshift of the Fe-His Mode and Its Slow Relaxation.** The frequency upshift of the Fe-His mode after CO photolysis is similar to that observed in previous work with high-probe-power, nanosecond pulses<sup>9,10,12,13</sup> and to that measured after photodissociation of O<sub>2</sub>.<sup>49</sup> On the basis of theoretical calculations by Stavrov,<sup>50</sup> Varotsis and Babcock<sup>49</sup> proposed that this change in the Fe-His frequency is related to the out-of-plane distance of the iron; an increase in this distance results in a lower Fe-His frequency. They excluded tilting of the histidine imidazole group, which has been proposed to explain similar Fe-His frequency changes in hemoglobin, because the predicted changes in the  $\nu_4$  mode<sup>50</sup> were not observed in CcO. The time scale of the Fe-His relaxation in

CcO is similar to that observed for tertiary structural relaxation in hemoglobin. In hemoglobin, however, this relaxation process is accompanied by changes in frequency of several heme modes. Since no heme mode frequency shifts occur on the nanosecond and microsecond time scale in CcO after photolysis,<sup>10,45</sup> we propose that the Fe-His relaxation is caused by a quaternary structural rearrangement of the protein. Moreover, we detect no significant perturbation of any heme modes at 5 ps after photolysis. Therefore, we conclude that an initial fast ( $\leq 5$  ps) relaxation occurs to a nonequilibrium geometry in which the iron is already out of the heme plane. Such a fast out-of-plane movement of the iron is in agreement with the work on hemoglobin and myoglobin.<sup>51,47b,c,38d</sup>

**Rb. sphaeroides.** Our data show that the photoproduct formed after CO photolysis in *Rb. sphaeroides* is similar to that in bovine CcO, i.e., heme  $a_3^{2+}$  with the proximal histidine as its axial ligand. The frequency of the Fe-His mode in the photoproduct is upshifted by 6 cm<sup>-1</sup>. This upshift is still present at 1 ns after photolysis (data not shown). It seems that CcO from *Rb. sphaeroides* shows the same  $\nu(\text{Fe-His})$  relaxation kinetics as bovine CcO, which is not surprising, given the similarities between the heme  $a_3$  pockets of both species.<sup>29,4</sup> We see no reason to assume that CO binds to heme  $a_3$  in two different conformations in a homogeneous native enzyme, as was suggested recently.<sup>52</sup> If CO were to bind in two different conformations, our data require that the heme  $a_3$  pocket rapidly relaxes within 50 ps to one uniform conformation following CO photolysis.

**Acknowledgment.** This work was supported by NIH Grant GM25480 and NATO Grant CRG 940275 (C.A.V.). We are grateful to Ms E. G. M. Vollenbroek, Dr. M. A. Pressler, and Mr. G. Pillot for the isolation of cytochrome oxidase and to Dr. Y. K. Kim for preliminary measurements.

JA964133P

(45) (a) Verkhovsky, M. I.; Morgan, J. E.; Wikström, M. *Biochemistry* **1992**, *31*, 11860–11863. (b) Verkhovsky, M. I.; Morgan, J. E.; Wikström, M. *Biochemistry* **1994**, *33*, 3079–3086.

(46) Einarsdóttir, Ó.; Dawes, T. D.; Georgiadis, K. E.; *Proc. Natl. Acad. Sci. U.S.A.* **1992**, *89*, 6934–6937.

(47) (a) Martin, J. L.; Migus, A.; Poyart, C.; Lecarpentier, Y.; Astier, R.; Antonetti, A. In *Ultrafast Phenomena*; Auston, P. H., Eisinger, K. B., Eds.; Springer: Berlin, 1984; Vol. IV, pp 447–451. (b) Martin, J. L.; Migus, A.; Poyart, C.; Lecarpentier, Y.; Astier, R.; Antonetti, A. *EMBO J.* **1983**, *2*, 1815–1819. (c) Martin, J. L.; Migus, A.; Poyart, C.; Lecarpentier, Y.; Antonetti, A. In *Hemoglobin*; Schnek, A. G., Paul, C., Eds.; University of Brussels: Brussels, 1984; pp 173–183. (d) Champion, P. *J. Raman. Spectrosc.* **1992**, *23*, 557–567.

(48) Nakashima, S.; Kitagawa, T. *J. Am. Chem. Soc.* **1994**, *116*, 10318–10319.

(49) Varotsis, C. A.; Babcock, G. T. *J. Am. Chem. Soc.* **1995**, *117*, 11260–11269.

(50) Stavrov, S. S. *Biophys. J.* **1993**, *65*, 1942–1950.

(51) Zhu, L.; Sage, J. T.; Champion, P. M. *Science* **1994**, *266*, 629–632.

(52) Wang, J.; Takahashi, S.; Hosler, J. P.; Mitchell, D. M.; Ferguson-Miller, S.; Gennis, R. B.; Rousseau, D. L. *Biochemistry* **1995**, *34*, 9819–9825.